Polymer Bulletin (2020) 77:5985–6003
https://doi.org/10.1007/s00289-019-03057-7

ORIGINAL PAPER

Electrospun tubes based on PLA, gelatin and genipin in different arrangements for blood vessel tissue engineering

Abraham Alejandro Leyva-Verduzco[1] · María Mónica Castillo-Ortega[1] · Lerma Hanaiy Chan-Chan[2] · Erika Silva-Campa[3] · Ramsés Galaz-Méndez[4] · Ricardo Vera-Graziano[5] · José Carmelo Encinas-Encinas[1] · Teresa Del Castillo-Castro[1] · Dora Evelia Rodríguez-Félix[1] · Hisila del Carmen Santacruz-Ortega[1] · Irela Santos-Sauceda[6]

Received: 19 June 2019 / Revised: 4 October 2019 / Accepted: 8 December 2019 /
Published online: 13 December 2019

Abstract

Four tubular membranes based on PLA and gelatin with different arrangements (PLA, gelatin, PLA-gelatin Blend and PLA/gelatin Core/Shell) were prepared by the electrospinning technique, the gelatin within the materials was crosslinked with genipin and all the meshes were characterized by SEM, ATR-FTIR, TGA, DSC, XRD and mechanical tests, also a viability essay and a confocal microscopy of HUVECs in contact with the materials were carried out. A 50% decrement of cellular viability was observed in the fibers with Core/Shell structure since the first day of culture compared with the tissue culture polystyrene, due to solubilization of non-crosslinked gelatin.

Keywords Electrospinning · Poly(lactic acid) · Gelatin · Tissue engineering

✉ María Mónica Castillo-Ortega
monicac@guaymas.uson.mx

[1] Departamento de Investigación en Polímeros y Materiales, Universidad de Sonora, 83000 Hermosillo Sonora, Mexico

[2] Departamento de Física, Universidad de Sonora, 83000 Hermosillo Sonora, Mexico

[3] Departamento de Investigación en Física, Universidad de Sonora, 83000 Hermosillo Sonora, Mexico

[4] GSE Biomedical, 83150 Hermosillo Sonora, Mexico

[5] Instituto de Investigaciones en Materiales, Universidad Nacional Autónoma de México, 04510 Ciudad de México, Mexico

[6] Centro de Investigación y de Estudios Avanzados Unidad Querétaro, 76230 Santiago de Querétaro, Querétaro, Mexico

Introduction

In order to solve the problems that generate some of the cardiovascular diseases, an invasive procedure known as artery bypass is used. In this intervention, the flow of blood is reflected using a vascular graft from a healthy place to another place where the blood is not nourishing the tissue due to an occlusion derived from an inflammatory process. For example, in the coronary artery bypass surgery, an autograft is commonly used to support the coronary artery system with blood from the aorta artery. The graft is usually the saphenous vein, the radial artery or the internal thoracic artery of the same patient [1, 2]. This involves, inconveniently, the necessity of another surgical intervention in order to extract the autograft [3]. To avoid a second surgical intervention, the autograft is replaced with a tube made of a biocompatible plastic material as Dacron and expanded Teflon. These materials have been used over the years, but when they are applied as small diameter blood vessel grafts (< 6 mm) they present some inconveniences; for example, aneurism formation, leaking, or change in diameter [4, 5]. Another strategy to solve the second intervention and enhance the quality of life of the patient is to use a tissue engineered system, in which a biocompatible and biodegradable scaffold with the shape of the graft serves as a physical medium, where cells can dwell and execute their functions such as attaching, proliferating, differentiating and secreting the components of the extracellular matrix required for creating new tissue [6, 7]. The electrospinning technique enables to generate fibrous matrices based on different polymers. This results convenient since the microstructured electrospun products can be obtained with tubular shapes and, at the same time, function as a cellular scaffold [8, 9].

Polylactic acid (PLA) is a biocompatible and biodegradable material that has been used in medical applications, i.e., as suture, surgical screws, drug delivery systems, among others [10]. Also, the PLA has been evaluated as polymer scaffold due to its processability and biodegradable characteristics; it is well known that the ability of PLA to interact with cells can be enhanced by using it in combination with better cellular host materials, for example, collagen, gelatin or polysaccharides [11–18]. Among them, gelatin is a product of the partial hydrolysis of collagen that has less immunogenic activity, which preserves integrin motifs that promote cellular adhesion and can be easily electrospun [16, 19–21]. Despite its qualities, gelatin gets solubilized by water, which is why a chemical crosslinking treatment is necessary to preserve the integrity of the manufactured materials. Genipin is a molecule found as a product of the gardenias fruit extraction. It is known that genipin can easily crosslink proteins, especially collagen and gelatin. Furthermore, it presents low toxicity compared with glutaraldehyde, diisocyanates and carbodiimides [22, 23].

With the purpose of mimicking the extracellular matrix in this study, fibrous tubes were manufactured by the electrospinning technique using the biocompatible polymers PLA and gelatin. In addition, a crosslinking treatment with genipin was applied to gelatin to avoid its solubilization. The novelty of this study is the comparative evaluation of the PLA and gelatin, both in blend and Core/Shell Arrangement. The behavior and viability of Human Umbilical Vein Endothelial Cells (HUVECs) was evaluated.

Materials and methods

Materials

PLA 2002D by Nature Works. Gelatin, gel strength 300, Type A from porcine skin, 2,2,2-trifluoroethanol and genipin were purchased from Sigma aldrich chemical Co.

Preparation of PLA, gelatin, PLA/gelatin-blended, PLA/gelatin Core–Shell structure membranes with a tubular shape using the electrospinning technique

The tubes were prepared by electrospinning technique using a 5-ml syringe (HENKE SASS WOLF. Model D-78532), a voltage source (SPELLMAN. Model CZE 1000R), a syringe pump (kdScientific. Model 2568CO) and a homemade 14 mm in diameter aluminum mandrel-type collector. 2,2,2-Trifluoroethanol was used as solvent and the solutions remained under magnetic stirring for 24 h before they were electrospun in all cases. The solution preparation process of each material is described below, and the electrospinning parameters are shown in Table 1.

For the PLA tubular membrane, a 14% w/v of PLA solution was prepared placing the solvent in a Pyrex storage bottle and adding the PLA pellets (previously minced in a blade mill) avoiding the cumulus of PLA formation. The gelatin tubular membrane was fabricated using a 14% w/v gelatin solution; it was prepared by placing the gelatin powder in a Pyrex storage bottle and carefully adding the solvent. For the PLA/gelatin-blended membrane, in a Pyrex storage bottle a 100:30 PLA and gelatin mix was hand shaken during 1 min before the solvent was added in a 14% PLA/solvent w/v ratio. The PLA/gelatin Core–Shell structure was fabricated using a PLA 14% w/v and a gelatin 14% w/v solution. Both solutions were added into different syringes and the Core–Shell arrangement was set with the PLA as core and gelatin as shell with a 23 G and a 13 G needles, respectively.

Crosslinking treatment of gelatin with genipin in the tubular membranes

The crosslinking treatment was carried out by placing each tubular membrane sample into a container and adding an amount of genipin 0.5% w/v ethanolic solution to reach a 4% in weight of geniping regarding the gelatin quantity for each of the

Table 1 Electrospinning parameters

Sample	Solvent	Voltage (kV)	Distance (cm)	Flow rate (mL min^{-1})	Concentration
PLA	TFE	15	12.5	10	14% w/v
Gelatin	TFE	15	16.5	10	14% w/v
Blended	TFE	11	15.5	10	14–4% w/w PLA-gelatin
Core–Shell	TFE	17	16.5	10/10 PLA-gelatin	14–14% w/v PLA-gelatin

TFE 2,2,2-trifluoroethanol

different tubular membrane samples. The culture tubes remained under mechanical agitation at 37 °C for 7 days, after that, the tubular membrane samples were rinsed three times with 3 ml of ethanol and dried in vacuum for 4 h. It can be observed in Fig. 1 how a sample change its color due to the reaction between gelatin and genipin [24]. The tubes that were treated with the crosslinker were named with a letter "C" at the beginning, CPLA, CGelatin, CCore/Shell and CBlend.

Scanning electron microscopy (SEM)

The microscopic morphology of the tubular membranes was observed using a scanning electron microscope (JEOL, model 5410LV) with a 20 kV accelerating voltage. A sputtered gold coating was placed onto each sample. The diameter fiber distribution was calculated using the software imageJ.

Transmission electronic microscopy (TEM)

The Core/Shell arrangement in the coaxial sample was observed using a transmission electron microscope JEOL 2010 F with a 200 kV accelerating voltage. The fibers of the samples were carefully taken from the tubular mesh using a pair of tweezers, and then, the fibers were placed between two grids in order to maintain them fixed during the essay.

Fourier transform infrared spectroscopy (FTIR)

With the purpose to observe whether the compounds of the materials were interacting between them, a FTIR analysis of the tubular membranes was carried out using a Frontier PerkinElmer FTIR/FIT spectrometer with an attenuated total reflectance (ATR) accessory. The samples were measured in the range of 4000–400 cm^{-1} with a resolution of 4 cm^{-1} in a transmittance mode.

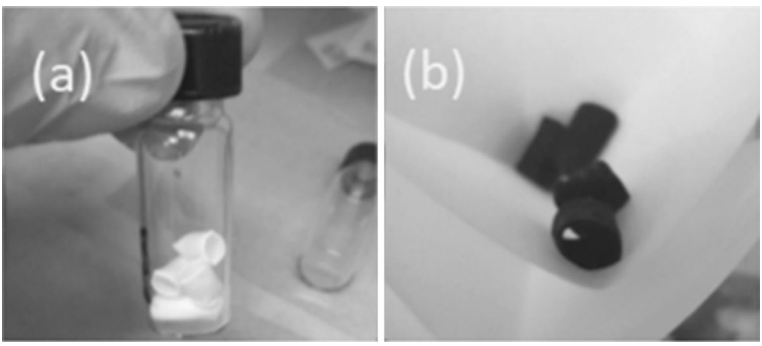

Fig. 1 Membranes before (**a**) and after (**b**) the crosslinking treatment

Thermogravimetric analysis (TGA)

The thermogravimetric analysis was carried out with the aim to examine whether the thermal stability of the materials was affected by the chemical interactions among its components and by the crosslinking treatment of gelatin. It was carried out using a PerkinElmer Pyris 1 TGA. 3 mg of each sample were weighed and placed in a platinum crucible; the experiment was performed by triplicate, within a temperature range of 25–900 °C at a 10 °C min^{-1} heat rate. All the analyses were executed under dry nitrogen atmosphere to avoid oxidation of the samples.

Differential scanning calorimetry (DSC)

A differential scanning calorimeter (PerkinElmer DSC 8500) was used to study the thermal transitions and the crosslinking reaction of the tubular membranes. Each specimen was weighted in range of 5–8 mg, sealed in an aluminum pan and scanned from 25 to 350 °C at a heat rate of 10 °C min^{-1} with a nitrogen flow of 20 ml min^{-1}.

X ray diffraction

An X-ray diffraction analysis was carried out in order to observe whether the crystalline structure of the PLA changed with the electrospinning and crosslinking process. To execute the analysis, the samples were cut in squares and analyzed with a Rigaku Dmax2100 diffractometer with Cu-Ni radiation ($\lambda = 1.54184$ Å) using a potential of 30 kV. The diffractograms were scanned within a range of 4–80° at a scan rate of 2° min^{-1}.

Mechanical analysis

In order to observe whether the materials have the characteristics to perform the functions of a blood vessel graft, they were subjected to different mechanical essays (longitudinal deformation, radial deformation and suture retention). The mechanical tests were carried out under tension by using an Instron ElectroPuls System E1000 using a load cell of 100 N and a deformation rate of 200 mm/min. To perform the tensile tests in the longitudinal direction of the tubes, the samples were cut to obtain a size of 50 mm of length. Two tempered steel adapters with a cylindrical shape and two clamps were used to assemble the samples.

To perform the tensile tests in the radial direction of the tubes, the tubular samples were cut 10 mm of length, two steel rods with 2 mm in diameter were placed through the lumen of the tube to clamp them into an aluminum hasp to be able of executing the deformation tests.

To calculate the suture retention, the tubes were cut in several 10 × 10 mm square samples, a suture was punctured 2 mm separated from the edge, the sample was fastened with a clamp, and the suture was held in a hook to execute the test.

Cell culture and cell viability essay

The HUVECs were cultured in DMEM medium at 37 °C with 5% of CO_2 pressure, supplemented with 10% of fetal bovine serum and 1% of penicillin streptomycin solution. The culture medium was changed every second day, and the cells were used at 4th to 5th subculture.

In the cell viability essay, the samples were placed into a 96 wells cell culture plate with an amount of 50 µL of a 70% ethanol aqueous solution to sterilize them. In the case of gelatin, the electrospun membrane was dissolved in the culture medium such that this medium was always used to simulate an indirect contact with the membrane. The essay started after the samples were rinsed during 4 days at 35 °C. 10,000 cells per well were seeded using supplemented DMEM and incubated at 37 °C with 5% of CO_2 pressure. The cell viability was measured by triplicate at days 1, 3 and 5. The culture medium was changed by a medium with resazurin; afterward, the samples were incubated by 4 h and read in a microplate reader at 570 and 600 nm. Equation 1 was used to calculate the cell viability where (ε), (A) and (C) represent the molar extinction coefficient, absorbance of the sample analyzed and absorbance of the cellular control, respectively. The subscript represents the wavelength of the measurement. Tissue culture polystyrene was used as control.

$$\text{Cell viability}\,(\%) = \left(\frac{\left(\varepsilon_{600} \times A_{570}\right) - \left(\varepsilon_{570} \times A_{600}\right)}{\left(\varepsilon_{600} \times C_{570}\right) - \left(\varepsilon_{570} \times C_{600}\right)} \right) \times 100 \tag{1}$$

Cell analysis by confocal microscopy

In order to observe the presence and shape of cells seeded on the manufactured materials, a 6 mm in diameter sample of each material was put within a well of a 44 wells microplate. To make sure that the seeded cells were interacting with the samples, an amount of 5000 cells in 50 µl of DMEM medium was carefully put onto the materials with the intention to form a drop above them. 2 h of incubation before adding 500 µl more DMEM medium were needed. Calcein AM was used to stain living cells, and the samples were observed using a confocal microscope Nikon A1R.

Statistical analysis of mechanical tests and biocompatibility

A one-way ANOVA was carried out using the software StatGraphics. Also, a Duncan's multiple range test was used for means comparison in both essays. In the mechanical analysis, the different letters "a, b, c" indicate that the difference of the

means is significant at the 0.05 level. In the biocompatibility tests, the star "*" indicates the groups statistically different ($p < 0.05$).

Results and discussion

Morphological analysis by SEM

Section (*k*) of Fig. 2 shows the scanning electron micrographs at 2000× of each of the samples before (left column) and after (right column) the crosslinking treatment. The membrane of PLA has a fibrous structure and an apparent smooth surface. On the other hand, the CPLA membrane presents a trend to shrink due to the contact with the polar solvents in the crosslinking system since there is no evidence of a chemical reaction between the PLA and genipin. The membrane of gelatin is composed by ribbons with a smooth appearance, after this membrane is crosslinked the ribbons structures tend to roll, and their surfaces are less smooth than in the sample before the crosslinking treatment. The Core/Shell membrane is composed by fibers with a smooth surface and minor diameter fibers are also found. The CCore/Shell membrane has a different structure than the non-crosslinked sample because the shell composed by gelatin broke and detached from the PLA core due to the stiffness of gelatin generated by the crosslinking reaction. The blend membrane has fibers with different sizes and with a semi-rough surface. The lack of miscibility between PLA and gelatin enables to see different tonalities in a simple fiber. For Cblend membrane, the tonalities of the fibers tend to homogenize and there are no unstructured parts as in the CCore/Shell membrane. Section (l) of Fig. 2 shows the diameter distribution of the samples PLA, gelatin, blend and Core/Shell. The fibers diameter distribution is leaning to the left for those materials that contain PLA. Conversely, the width distribution of the ribbons of gelatin sample tends to lean to the right. A wide standard deviation is found in the distribution of PLA because the population extends to big fibers.

Analysis of Core/Shell structure by TEM

Figure 3 shows a TEM micrography of a single fiber of the coaxial sample. The Core/Shell structure can be observed, and it is indicated by two arrows. There is another arrow that indicates a part of the grid in which the sample was fixed.

Chemical analysis by FTIR

The ATR-FTIR spectra of the membranes PLA, gelatin, Core/Shell and blend are shown in section (a) of Fig. 4. The characteristic stretch vibrations of the carbonyl group band (C=O) and (C–O) bond of the ester structure in the backbone of PLA appears at 1755 cm^{-1} and 1183 cm^{-1} [25, 26]. In the IR spectrum of the membrane gelatin, three main signals of the functional group amide (CONH) can be found, usually named as amide I (1633 cm^{-1}, corresponding to the stretch of the functional

Fig. 2 Section (*k*) scanning electron microscopy at 2000× of the samples **a** PLA, **b** CPLA, **c** gelatin, **d** ▶ CGelatin, **e** Core/Shell, **f** CCore/Shell, **g** blend and **h** CBlend. Section **l** fiber diameter distribution of the samples PLA, gelatin, Core/Shell and blend samples

group C=O with contributions of CN, CCN and NH) amide II (1533 cm^{-1} corresponding to NH scissoring and CN out of phase vibration with contributions of CO and CC) and amide III (1444 cm^{-1} corresponding to vibrations NH and CN) [27, 28]. On the other hand, the band amide I in the spectrum of the membranes Core/Shell and blend shifted from 1633 to 1638 cm^{-1} and 1650 cm^{-1}, respectively. This indicates an interaction between the PLA and gelatin for the case of both membranes, regarding the Core/Shell and blend spectra the carbonyl group signal of PLA (C=O) shifted to lower energy in both cases whereas a hydrogen bond interaction between the carbonyl groups of PLA and the hydrogen of the N–H bond in the amide groups of the backbone structure of the gelatin. A graphic representation of the interaction between PLA and gelatin is shown in section (b) of Fig. 4 [26]. Moreover, if the carbonyl group (C=O) of the PLA compound (1755 cm^{-1}) is taken as a reference, the intensity of the amide signals of the gelatin is higher in the spectrum of the Core/Shell than in the spectrum of blend membrane since the amount of gelatin used in its composition, 50 and 30% in weight, respectively.

The section (a) of Fig. 5 shows the ATR-FTIR spectra of the membranes gelatin and CGelatin. In the CGelatin spectrum, two new bands can be observed; one for the carbonyl group (C=O) corresponding to genipin structure at 1732 cm^{-1} and another band at 1045 cm^{-1} corresponding to a (CN) [27, 29] amine vibration product of a chemical reaction between gelatin and genipin, as it is represented in the section (b) of Fig. 5 [30, 31]. In summary, through ATR-FTIR the hydrogen bond among PLA and gelatin and the crosslinking reaction of gelatin can be confirmed.

Although the application of the materials does not pretend to be at high temperatures, the analysis was performed in order to know whether the crosslinking reaction caused any alteration in the thermal profiles of the samples. Figure 6 shows the TGA curves of all the fibrous samples PLA and CPLA (a), gelatin and CGelatin (b), Core/Shell and CCore/Shell (c), and finally, Blend and CBlend (d). The complete set of experiments were carried out 4 h after the samples were dried with vacuum at room temperature. Almost all the materials except the PLA presented a first step around 100 °C as a result of the presence of water. As expected, the pure gelatin-based materials (b) are the most hygroscopic samples and the amount of water within them is 10% in both cases before and after being crosslinked. The Core/Shell and blend samples detained around 5% of water before and after the crosslinking treatment. The thermogravimetric profile of PLA and CPLA are compounded only by one step with a maximum rate at 364.6 ± 0.4 and 363.9 ± 1.3 °C, respectively. The degradation of the gelatin and CGelatin samples consist on three steps: The first one as a consequence of the presence of water as it was mentioned before; the second step was found at 330.9 ± 0.7 and 330.6 ± 0.4 °C for both, due to hydrolysis and oxidation [33], and the last one at 755.2 ± 10 and 778.2 ± 20 °C, respectively. The TGA curve for the Core/Shell, CCore/Shell samples are composed by three steps with the PLA degradation step at 339.7 ± 5.7, 347.8 ± 2.2 °C. A similar profile was found for

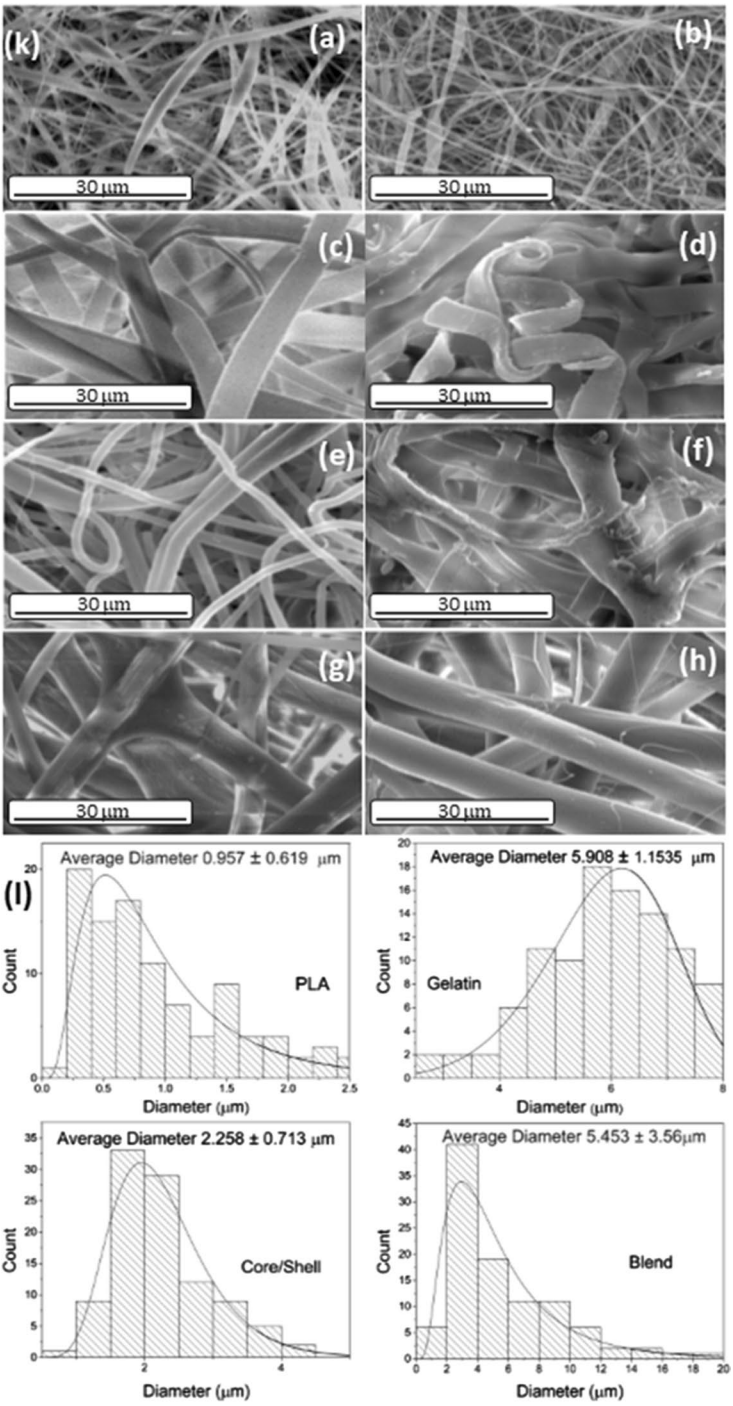
(k)
(a)
30 μm
(b)
30 μm
(c)
30 μm
(d)
30 μm
(e)
30 μm
(f)
30 μm
(g)
30 μm
(h)
30 μm
(l)
Average Diameter 0.957 ± 0.619 μm
PLA
Count
Diameter (μm)
Average Diameter 5.908 ± 1.1535 μm
Gelatin
Count
Diameter (μm)
Average Diameter 2.258 ± 0.713 μm
Core/Shell
Count
Diameter (μm)
Average Diameter 5.453 ± 3.56μm
Blend
Count
Diameter (μm)

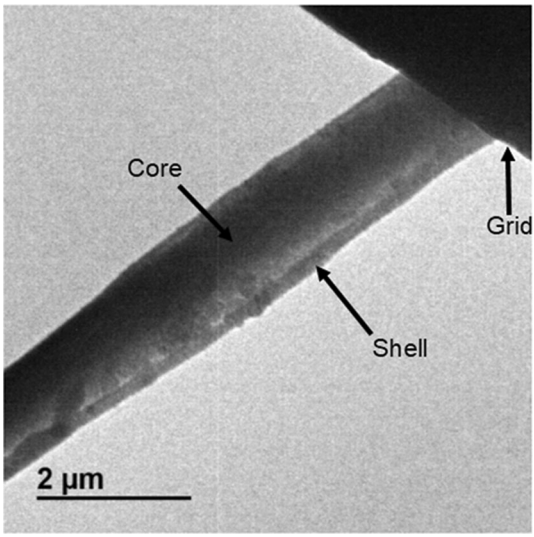

Fig. 3 TEM micrography of a single fiber of the coaxial sample

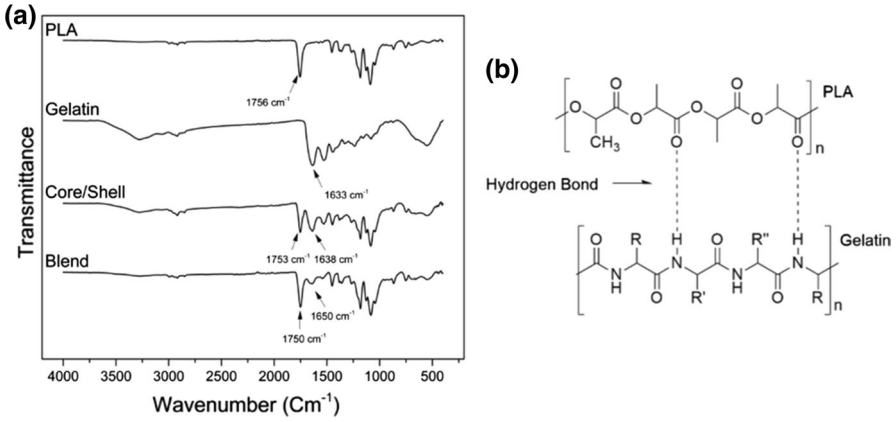

Fig. 4 **a** ATR-FTIR spectra of the membranes PLA, gelatin, Core/Shell and blend. **b** Molecular representation of the interaction between PLA and gelatin

the blend and CBlend samples with the PLA degradation step at 345.8 ± 2.3 and 345.1 ± 1.8 °C, respectively. No significant changes were found in the loss of mass steps by cause of crosslinking treatment. It was validated by a one-way ANOVA and a Duncan's multiple range test ($p < 0.05$).

Thermal Transitions by DSC Analysis

Figure 7 shows the DSC thermograms of the samples PLA and CPLA (a), gelatin and CGelatin (b), Core/Shell and CCore/Shell (c) and Blend and CBlend (d). The PLA thermogram presents two endothermic peaks; the first peak corresponds to

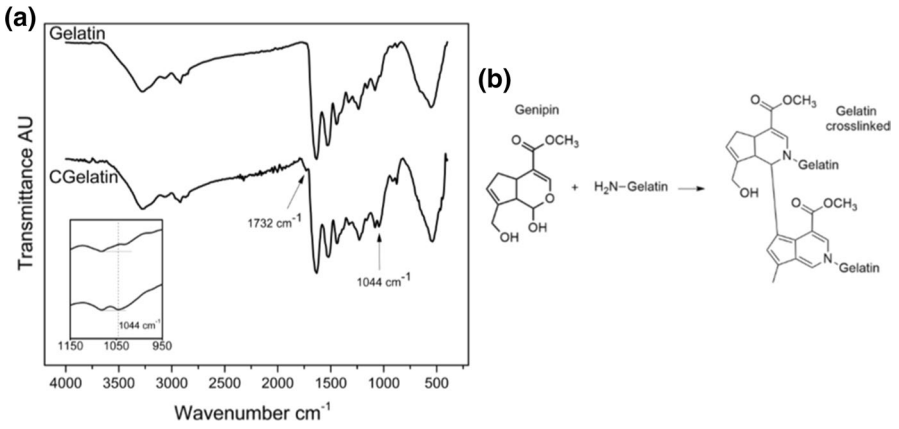

Fig. 5 **a** ATR-FTIR spectra of the membranes gelatin and CGelatin. **b** Molecular representation of the crosslinking reaction between PLA and gelatin [30–32]

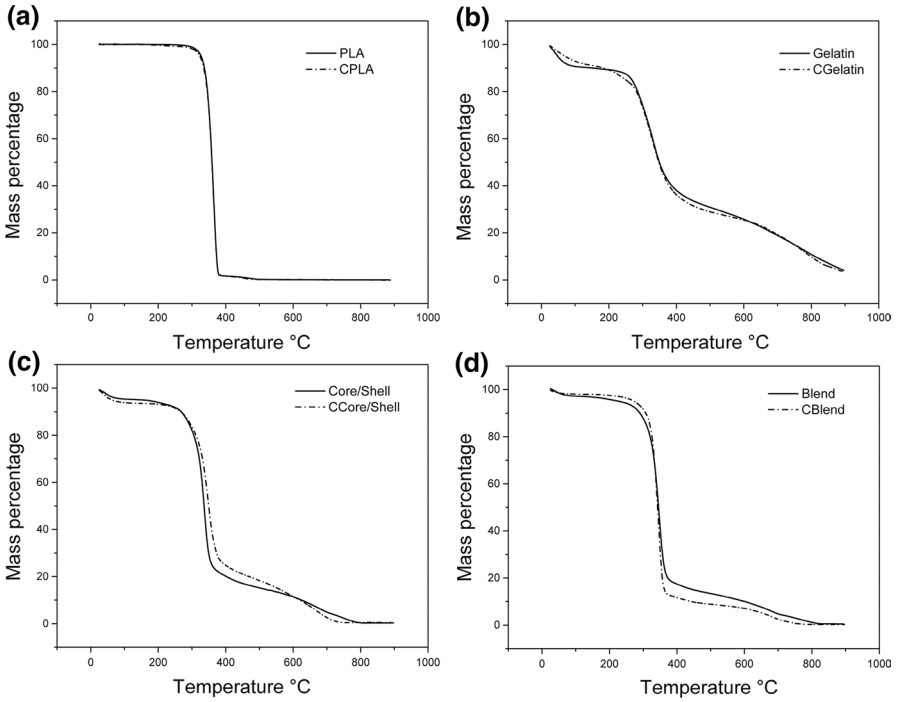

Fig. 6 TGA curves of the samples PLA and CPLA (**a**), gelatin and CGelatin (**b**), Core/Shell and CCore/Shell (**c**) and blend and CBlend (**d**)

a glass transition (T_g) at 74 °C and the second signal represents a melting transition [34] (T_m) at 165 °C while the curve of CPLA does not present the T_g transition due to the presence of the genipin between the backbone of PLA. This is

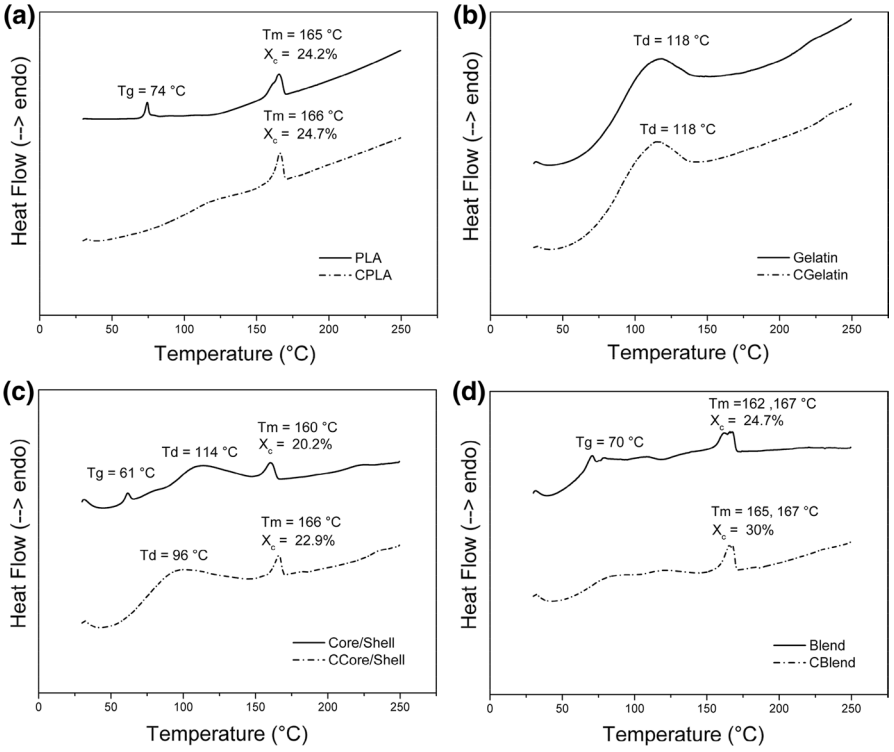

Fig. 7 DSC thermograms of the tubes PLA, CPLA (**a**), gelatin, CGelatin (**b**), Core/Shell, CCore/Shell (**c**) and blend, CBlend (**d**)

because the genipin reacts with primary amine groups. The gelatin membrane presents a wide denaturalization transition (T_D) [35] with a maximum heat flow at 118 °C that did not change when it is treated with genipin, in contrast to the crosslinking with glutaraldehyde that shifted it 10 °C [35]. The DSC curve of the Core/Shell structure shows the transition temperatures of each of its components. In the case of the blend sample, there is not a notorious gelatin T_d because the interaction between the materials led to the denaturalization of the protein. The PLA T_g of Core/Shell and blend indicates an interaction between its components since it decreased 13 and 4 °C, respectively, to a lower temperature compared with the pure PLA material [36]. When the materials are treated with genipin, the PLA glass transition disappears for all the cases indicating that the backbone of the PLA did not relax to the crosslinking. Also, in the sample CCore/Shell, the denaturalization temperature of gelatin shifts to a lower temperature as product of the crosslinking reaction. On the other hand, DSC analysis was applied to calculate the melting heat and crystallinity (X_c) of PLA [37]. It was possible to observe a correlation between the crystallinity of PLA in the samples treated and non-treated with genipin. The X_c of PLA in the CBlend and CCore/Shell materials are higher than those in blend and Core/Shell materials. This shows that the

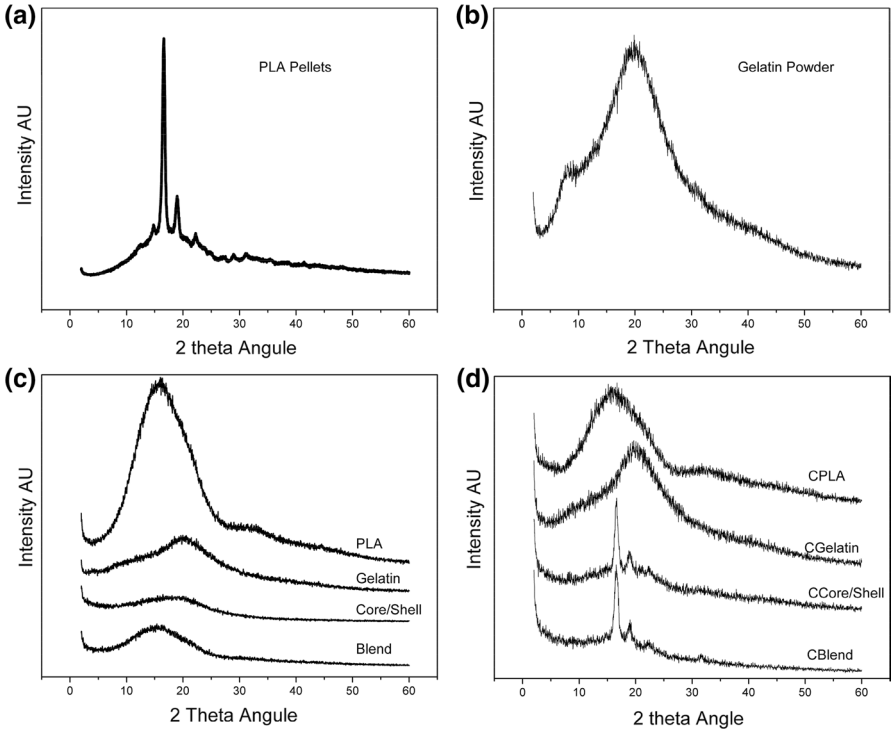

Fig. 8 **a** XRD patterns of PLA pellets, **b** XRD patterns of gelatin powder, **c** XRD patterns of the samples PLA, gelatin, Core/Shell, blend, **d** XRD patterns of the samples CPLA, CGelatin, CCore/Shell, CBlend

crystalline phase of PLA has increased for those materials that have been treated with the crosslinker. It can also be associated with the emergence of the PLA crystal pattern in the XRD analysis in Fig. 8. This pattern does not appear when the crosslinking treatment is applied to the PLA membrane, which suggests that the crosslinking of gelatin is the cause of PLA crystallization.

Analysis of crystallinity by XRD

The XRD pattern of the raw PLA material and gelatin are, respectively, shown in the section (a) and (b) of Fig. 8. The section (c) shows the samples PLA, gelatin, Core/Shell and blend, and the section (d) shows the CPLA, CGelatin, CCore/Shell and CBlend samples. The PLA before being electrospun shows a semicrystalline structure with peaks at 16.56° and 19.01° (Bragg's angle) [38, 39]. In the electrospun samples PLA, gelatin, Core/Shell and blend (c) an amorphous XRD pattern for all the samples is found, while the CCore/Shell and CBlend samples (d) showed again the semicrystalline phase seen in PLA pellets. This suggests that the process of electrospinning unpacks the crystalline structure of PLA because it must be dissolved in order to carry out the electrospinning process. On the other hand, the gelatin

crosslinking modifies the gelatin arrangement and promotes a self-assembling of PLA.

Mechanical properties of tubular membranes under tensile and radial stresses

Although gelatin was used as a component in the manufactured materials, these did not present semi-interpenetrating polymer network behavior. Table 2 shows the mechanical properties of the crosslinked samples. The sample CGelatin could not be analyzed because it lost its tubular shape after the crosslinking reaction. The CBlend material showed the highest elastic modulus with a value of 67.8 ± 2.1 kPa in radial strain (RS) and 526 ± 78 kPa in longitudinal strain (LS) followed by the CCore/Shell sample with an elastic modulus of 24.5 ± 2.5 kPa (RS) and 18.9 ± 118.8 kPa (LS). Ultimately, the PLA sample presented values of 12.2 ± 0.34 kPa (RS) and 170 ± 40 kPa (LS). The high modulus of CBlend compared with CCore/Shell can be justified by the reduction in crystallinity by cause of the chemical interactions between PLA and gelatin. In case of the yield stress, the circumferential stress of CBlend showed a higher stress than CCore/Shell and PLA. On the other hand, in the longitudinal essay analogous stress values were obtained for CBlend and PLA. The failure strain of PLA in the circumferential and longitudinal essay is higher than those of CCore/Shell and CBlend due to the stiffness acquired by combining the polymers and the crosslinking treatment. The Cblend presented the lowest value of suture retention (85.96 ± 3.16 gf) while a similar behavior was found for the PLA and CCore/Shell stress with a value of 170.09 ± 9.89 and 169.37 ± 22.74 gf, respectively. In summary, although the mechanical properties of the electrospun materials are below of those for a blood vessel [40], they can be modified by decreasing the fiber diameter [41]. CBlend presented higher mechanical properties compared with CCore/Shell, and this can be justified by the chemical interactions of the materials. In the CBlend mesh, the PLA and gelatin are interacting in the whole fibers structures while in the CCore/Shell sample the chemical interactions are only presented in the interface of the Core/Shell fiber structure.

Table 2 Summary of mechanical characteristic of tubular membranes

	PLA	CCore/Shell	CBlend
Elastic modulus (KPa)	$^{a}12.2 \pm 0.34$ RS[1]	$^{b}24.5 \pm 2.5$ RS	$^{c}67.8 \pm 2.1$ RS
	$^{a}170 \pm 40$ LS[2]	$^{a}118.9 \pm 11.8$ LS	$^{b}526 \pm 78$ LS
Yield point (KPa)	$^{a}340. \pm 11$ RS	$^{a}308.3 \pm 21.8$ RS	$^{b}982 \pm 80$ RS
	$^{a}2520 \pm 390$ LS	$^{b}1370 \pm 360$ LS	$^{b}2320 \pm 390$ LS
Elongation to failure (%)	$^{a}104.96 \pm 2.61$ RS	$^{b}32.22 \pm 5.13$ RS	$^{c}49.4 \pm 3.5$ RS
	$^{a}103.46 \pm 5.77$ LS	$^{b}39.45 \pm 3.25$ LS	$^{b}15.0 \pm 3.1$ LS
Suture retention (Gf)	$^{a}170.09 \pm 9.89$	$^{a}85.96 \pm 3.16$	$^{b}169.37 \pm 22.74$

[1]Radial Strain. [2]Longitudinal Strain. ANOVA and Duncan's multiple range test were carried out using the software StatGraphics

[a, b, c]Indicate that the difference of the means is significant at the 0.05 level

Cellular viability analysis by resazurin reduction essay

In order to compare the ability of PLA and gelatin-based materials to act as cellular host, a cellular viability essay was carried out using HUVECs. The physical characteristics of CGelatin sample prevent to carry out this analysis. In the bar plot section (a) in Fig. 9, it can be observed the cellular viability of HUVECs interacting with the single PLA and single gelatin materials. In the case of the gelatin membrane, it was dissolved in the culture medium and the cells were seeded on the tissue culture polystyrene. The cellular viability remained above 80% until 5 days of culture which suggest that the materials do not present a toxic behavior. Section (b) of Fig. 9 shows the bar plot of the viability of HUVECs seeded on the Blend, CBlend, Core/Shell and CCore/Shell materials. It can be observed that the cellular activity decreased below 75% since the first day for the Core/Shell arrangement samples while the Blend samples it kept over 80%, the CCore/Shell sample presented more cellular viability than the non-treated sample. This suggests that the low cellular viability on the Core/Shell materials could be attributed to the solubility characteristic of gelatin.

Cellular analysis by confocal microscopy

Figure 10 shows confocal micrographs of HUVECs after 24 h of seeding onto the Core/Shell, CCore/Shell, Blend and CBlend membranes. The cells on the Core/Shell sample show a circular morphology indicating a weak capacity of adherence while in the CCore/Shell structure the cells are trending to spreading out. On the other hand, the cells seeded onto the Blend and CBlend samples showed a greater outstretched morphology following the fibers. The trend to outstretching is more notorious in the blend and in the crosslinked samples because the gelatin remains in the structure [42] and do not eventually dissolves as it is indicated by the decrease in the amine I and amine II band around 1630 and 1530 cm^{-1}, respectively, shown in the ATR-FTIR spectra as shown in Fig. 11.

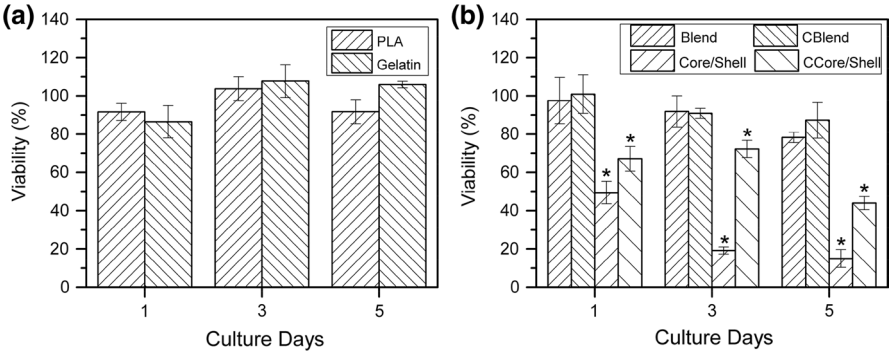

Fig. 9 Bar plot of cellular viability of HUVECs in contact with the samples **a** PLA and gelatin, **b** blend, CBlend, Core/Shell and CCore/Shell. ANOVA and Duncan's multiple range test were carried out using the software StatGraphics. The asterisk (*) indicates the groups statistically different ($p < 0.05$)

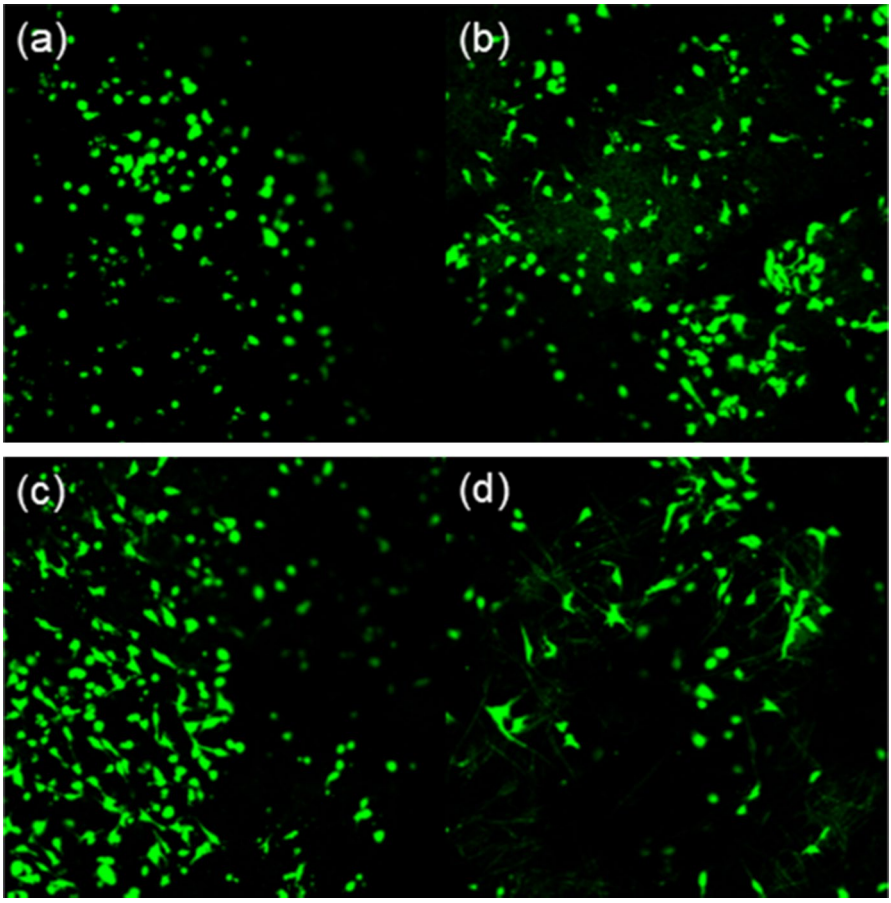

Fig. 10 Confocal micrographs of HUVECs stained with calcein AM resting on the samples **a** Core/Shell, **b** CCore/Shell, **c** blend and **d** CBlend

Conclusions

Eight different fibrous tubes based on PLA, gelatin and genipin were obtained. The SEM analysis revealed the fibrous morphology of the membranes that mimicks the extracellular matrix of soft tissues, suggesting potential benefits for some tissue engineering applications. The FTIR and DSC analysis suggested a hydrogen bond interaction among the PLA and gelatin. Furthermore, a band indicating the formation of a tertiary amine due to the gelatin crosslinking reaction was found. The viability of HUVECs in contact with the materials remained around 80% until day 5 of culture for the case of PLA, gelatin and blend samples while in the Core/Shell structure this gone down to 60% since the first day of culture, indicating that the solubility of gelatin in the material was not beneficent to retain

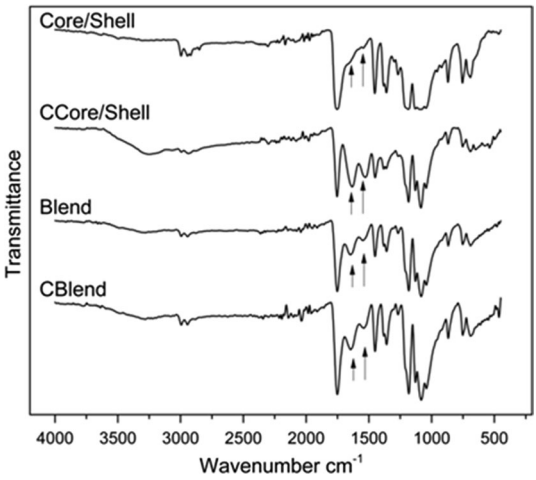

Fig. 11 ATR-FTIR spectra of Core/Shell, CCore/Shell, blend and CBlend samples after 5 days of cellular culture

HUVECs on its matrix. The blend and CBLend samples are good materials with potential application as scaffold in cell culture.

References

1. Cameron A, Davis KB, Green G, Schaff HV (1996) Coronary bypass surgery with internal-thoracic-artery grafts—effects on survival over a 15-year period. N Engl J Med 334(4):216–220. https://doi.org/10.1056/NEJM199601253340402
2. Gaudino M, Benedetto U, Fremes S et al (2018) Radial-artery or saphenous-vein grafts in coronary-artery bypass surgery. N Engl J Med 378(22):2069–2077. https://doi.org/10.1056/nejmoa1716026
3. Serruys PW, Unger F, Sousa JE et al (2001) Comparison of coronary-artery bypass surgery and stenting for the treatment of multivessel disease. N Engl J Med 344(15):1117–1124. https://doi.org/10.1056/NEJM200104123441502
4. Awad NK, Niu H, Ali U, Morsi YS, Lin T (2018) Electrospun fibrous scaffolds for small-diameter blood vessels: a review. Membranes (Basel). 8(1):1–26. https://doi.org/10.3390/membranes8010015
5. Kharazi AZ, Atari M, Vatankhah E, Javanmard SH (2018) A nanofibrous bilayered scaffold for tissue engineering of small-diameter blood vessels. Polym Adv Technol 29(12):3151–3158. https://doi.org/10.1002/pat.4437
6. Raines EW (2000) The extracellular matrix can regulate vascular cell migration, proliferation, and survival: relationships to vascular disease. Int J Exp Pathol. 81(3):173–182
7. Heydarkhan-Hagvall S, Schenke-Layland K, Dhanasopon AP et al (2008) Three-dimensional electrospun ECM-based hybrid scaffolds for cardiovascular tissue engineering. Biomaterials 29(19):2907–2914. https://doi.org/10.1016/j.biomaterials.2008.03.034
8. Kai D, Liow SS, Loh XJ (2015) Biodegradable polymers for electrospinning: towards biomedical applications. Mater Sci Eng, C 45:659–670. https://doi.org/10.1016/j.msec.2014.04.051
9. Strobel HA, Calamari EL, Beliveau A, Jain A, Rolle MW (2018) Fabrication and characterization of electrospun polycaprolactone and gelatin composite cuffs for tissue engineered blood vessels. J Biomed Mater Res—Part B Appl Biomater 106(2):817–826. https://doi.org/10.1002/jbm.b.33871
10. Tsuji H (2014) Poly (lactic acid). https://doi.org/10.1002/9780470649848
11. Park H, Radisic M, Lim JO, Chang BH, Vunjak-Novakovic G (2005) A novel composite scaffold for cardiac tissue engineering. Vitr Cell Dev Biol Anim. 41(7):188. https://doi.org/10.1290/0411071.1
12. Mi HY, Jing X, Li ZT, Lin YJ, Thomson JA, Turng LS (2019) Fabrication and modification of wavy multicomponent vascular grafts with biomimetic mechanical properties, antithrombogenicity,

and enhanced endothelial cell affinity. J Biomed Mater Res Part B Appl Biomater 1–12. https://doi.org/10.1002/jbm.b.34333
13. Swarnalatha B, Nair SL, Shalumon KT et al (2013) Poly (lactic acid)-chitosan-collagen composite nanofibers as substrates for blood outgrowth endothelial cells. Int J Biol Macromol 58:220–224. https://doi.org/10.1016/j.ijbiomac.2013.03.060
14. Lynn AK, Yannas IV, Bonfield W (2004) Antigenicity and immunogenicity of collagen. J Biomed Mater Res Part B Appl Biomater 71(2):343–354. https://doi.org/10.1002/jbm.b.30096
15. Krebsbach PH, Mankani MH, Satomura K, Kuznetsov SA, Robey PG (1998) Repair of craniotomy defects using bone marrow stromal cells. Transplantation 66(10):1272–1278. https://doi.org/10.1097/00007890-199811270-00002
16. Peter M, Binulal NS, Nair SV, Selvamurugan N, Tamura H, Jayakumar R (2010) Novel biodegradable chitosan-gelatin/nano-bioactive glass ceramic composite scaffolds for alveolar bone tissue engineering. Chem Eng J 158(2):353–361. https://doi.org/10.1016/j.cej.2010.02.003
17. Dreesmann L, Ahlers M, Schlosshauer B (2007) The pro-angiogenic characteristics of a cross-linked gelatin matrix. Biomaterials 28(36):5536–5543. https://doi.org/10.1016/j.biomaterials.2007.08.040
18. Hong Y, Gong Y, Gao C, Shen J (2008) Collagen-coated polylactide microcarriers/chitosan hydrogel composite: injectable scaffold for cartilage regeneration. J Biomed Mater Res Part A. 85(3):628–637. https://doi.org/10.1002/jbm.a.31603
19. Aldana AA, Abraham GA (2017) Current advances in electrospun gelatin-based scaffolds for tissue engineering applications. Int J Pharm 523(2):441–453. https://doi.org/10.1016/j.ijpharm.2016.09.044
20. Ullm S, Krüger A, Tondera C et al (2014) Biocompatibility and inflammatory response in vitro and in vivo to gelatin-based biomaterials with tailorable elastic properties. Biomaterials 35(37):9755–9766. https://doi.org/10.1016/j.biomaterials.2014.08.023
21. Piris MA, Mollejo M, Campo E, Menárguez J, Flores T, Isaacson PG (1998) A marginal zone pattern may be found in different varieties of non-Hodgkin's lymphoma: the morphology and immunohistology of splenic involvement by B-cell lymphomas simulating splenic marginal zone lymphoma. Histopathology 33(3):230–239. https://doi.org/10.1046/j.1365-2559.1998.00478.x
22. Manickam B, Sreedharan R, Elumalai M (2014) 'Genipin'—the natural water soluble cross-linking agent and its importance in the modified drug delivery systems: an overview. Curr Drug Deliv 11(1):139–145. https://doi.org/10.2174/15672018113106660059
23. Liang HC, Chang WH, Liang HF, Lee MH, Sung HW (2004) Crosslinking structures of gelatin hydrogels crosslinked with genipin or a water-soluble carbodiimide. J Appl Polym Sci 91(6):4017–4026. https://doi.org/10.1002/app.13563
24. Butler MF, Ng YF, Pudney PDA (2003) Mechanism and kinetics of the crosslinking reaction between biopolymers containing primary amine groups and genipin. J Polym Sci, Part A: Polym Chem 41(24):3941–3953. https://doi.org/10.1002/pola.10960
25. Wang DK, Varanasi S, Fredericks PM et al (2013) FT-IR characterization and hydrolysis of PLA-PEG-PLA based copolyester hydrogels with short PLA segments and a cytocompatibility study. J Polym Sci, Part A: Polym Chem 51(24):5163–5176. https://doi.org/10.1002/pola.26930
26. 2001—Thomson Learning, Inc.—Pavia, Lampman, Kriz - Introduction to Spectroscopy third edition.pdf
27. Hashim DM, Man YBC, Norakasha R, Shuhaimi M, Salmah Y, Syahariza ZA (2010) Potential use of Fourier transform infrared spectroscopy for differentiation of bovine and porcine gelatins. Food Chem 118(3):856–860. https://doi.org/10.1016/j.foodchem.2009.05.049
28. Daniel-Da-Silva AL, Salgueiro AM, Trindade T (2013) Effects of Au nanoparticles on thermoresponsive genipin-crosslinked gelatin hydrogels. Gold Bull. 46(1):25–33. https://doi.org/10.1007/s13404-012-0078-1
29. Barth A (2007) Infrared spectroscopy of proteins. Biochim Biophys Acta Bioenerget 1767(9):1073–1101. https://doi.org/10.1016/j.bbabio.2007.06.004
30. Di Tommaso S, David H, Gomar J, Leroy F, Adamo C (2014) From iridoids to dyes: a theoretical study on genipin reactivity. RSC Adv 4(22):11029–11038. https://doi.org/10.1039/c3ra47159d
31. Touyama R, Takeda Y, Inoue K et al (2011) Studies on the blue pigments produced from genipin and methylamine. I. Structures of the brownish-red pigments, intermediates leading to the blue pigments. Chem Pharm Bull 42(3):668–673. https://doi.org/10.1248/cpb.42.668
32. Devi N, Maji TK (2010) Genipin crosslinked microcapsules of gelatin a and κ-carrageenan polyelectrolyte complex for encapsulation of neem (*azadirachta indica* a.juss.) seed oil. Polym Bull 65(4):347–362. https://doi.org/10.1007/s00289-010-0246-5

33. Moshiul Alam AKM, Beg MDH, Mina MF, Mamun AA, Bledzki AK (2015) Degradation and stability of green composites fabricated from oil palm empty fruit bunch fiber and polylactic acid: effect of fiber length. J Compos Mater 49(25):3103–3114. https://doi.org/10.1177/0021998314560219
34. Frone AN, Berlioz S, Chailan JF, Panaitescu DM (2013) Morphology and thermal properties of PLA-cellulose nanofibers composites. Carbohydr Polym 91(1):377–384. https://doi.org/10.1016/j.carbpol.2012.08.054
35. Jalaja K, Naskar D, Kundu SC, James NR (2015) Fabrication of cationized gelatin nanofibers by electrospinning for tissue regeneration. RSC Adv 5(109):89521–89530. https://doi.org/10.1039/c5ra10384c
36. Feldstein MM, Roos A, Chevallier C, Creton C, Dormidontova EE (2003) Relation of glass transition temperature to the hydrogen bonding degree and energy in poly(N-vinyl pyrrolidone) blends with hydroxyl-containing plasticizers: 3. Analysis of two glass transition temperatures featured for PVP solutions in liquid poly(ethyle). Polymer Guildf 44(6):1819–1834. https://doi.org/10.1016/s0032-3861(03)00046-6
37. Bouakaz BS, Pillin I, Habi A, Grohens Y (2018) Synergy between fillers in organomontmorillonite/graphene-PLA nanocomposites. Appl Clay Sci 2015(116–117):69–77. https://doi.org/10.1016/j.clay.2015.08.017
38. Mathew AP, Oksman K, Sain M (2006) The effect of morphology and chemical characteristics of cellulose reinforcements on the crystallinity of polylactic acid. J Appl Polym Sci 101(1):300–310. https://doi.org/10.1002/app.23346
39. Inai R, Kotaki M, Ramakrishna S (2005) Structure and properties of electrospun PLLA single nanofibres. Nanotechnology 16(2):208–213. https://doi.org/10.1088/0957-4484/16/2/005
40. Ercolani E, Del Gaudio C, Bianco A (2013) Vascular tissue engineering of small-diameter blood vessels: reviewing the electrospinning approach. J Tissue Eng Regen Med 2012:861–888. https://doi.org/10.1002/term
41. Wong SC, Baji A, Leng S (2008) Effect of fiber diameter on tensile properties of electrospun poly(ε-caprolactone). Polymer (Guildf). 49(21):4713–4722. https://doi.org/10.1016/j.polymer.2008.08.022
42. Huang Y, Onyeri S, Siewe M, Moshfeghian A, Madihally SV (2005) In vitro characterization of chitosan-gelatin scaffolds for tissue engineering. Biomaterials 26(36):7616–7627. https://doi.org/10.1016/j.biomaterials.2005.05.036